

Single-particle spectra of charge-transfer insulators by cluster perturbation theory: The correlated band structure of NiO

R. Eder,¹ A. Dorneich,² and H. Winter¹¹Forschungszentrum Karlsruhe, Institut für Festkörperphysik, 76021 Karlsruhe, Germany²IBM Deutschland Entwicklung GmbH, 71032 Böblingen, Germany

(Received 18 August 2004; published 7 January 2005)

We propose a many-body method for band-structure calculations in strongly correlated electron systems and apply it to NiO. The method may be viewed as a translationally invariant version of the cluster method of Fujimori and Minami. Thereby the Coulomb interaction within the d -shells is treated by exact diagonalization and the d -shells then are coupled to a solid by an extension of the cluster perturbation theory due to Senechal *et al.* The method is computationally no more demanding than a conventional band structure calculation and for NiO we find good agreement between the calculated single particle spectral function and the experimentally measured band structure.

DOI: 10.1103/PhysRevB.71.045105

PACS number(s): 72.80.Ga, 71.27.+a, 79.60.-i

I. INTRODUCTION

Band structure calculations based on the single-particle picture have enjoyed considerable success in solid state theory. Single-particle picture here is meant to imply that the ground state is obtained by filling up according to the Pauli principle the energy levels calculated for a single electron in an “effective potential.” The effective potential thereby is usually constructed within the framework of the local density (LDA) or local spin density approximation (LSDA) to density functional theory (DFT)¹ and despite the well-known fact that the eigenvalues of the Kohn-Sham equations should not be identified with the single-particle excitation energies of a system, the resulting band structures often give an almost quantitative description of angle-resolved photoemission spectroscopy (ARPES).

However, there are also some classes of solids which defy such a description, most notably transition metal compounds with partially filled d - and f -shells and strong Coulomb interaction between the electrons in these. A frequently cited example is NiO, where LSDA band structure calculations correctly predict an antiferromagnetic and insulating ground state, but only a small “Slater gap” of a fraction of an eV,² whereas experimentally NiO is an insulator with a band gap of 4.3 eV³ and stays so even above the magnetic ordering temperature. While DFT thus gives reasonable answers within its domain of validity—namely ground state properties—the noncorrespondence between the Kohn-Sham eigenvalues and the single-particle excitation energies of the solid obviously has to be taken literal for this compound (if the band gap is not read off from the LSDA band structure but expressed as the difference of ground state energies it is in fact possible to calculate it within the framework of DFT, as shown by Norman and Freeman⁴). It is generally believed that the reason for the discrepancy is the strong Coulomb interaction between the electrons in the Ni $3d$ -shell, which leads to a substantial energy splitting between d^n configurations with different n . This leads to a very pronounced “pinning” of the d -shell occupation number n , in the case of NiO to the value $n=8$. Final states for photoemission or inverse

photoemission then correspond to a single d -shell being in either a d^7 , a d^8 , or a d^9 configuration, in each case with very small admixture of configurations with other n . The corresponding “defect” then may be thought of propagating through the crystal with definite \mathbf{k} . This pinning of the electron number in both initial and final states cannot be reproduced by a wave function which takes the form of a simple Slater-determinant, such as the ground state deduced from the Kohn-Sham equations. The situation is improved somewhat in the selfinteraction corrected version of DFT,^{5,6} which renders a certain fraction of the d -orbitals completely localized, so that their occupation number in fact does become pinned—for the remaining delocalized d -orbitals, however, the problem remains. Another way to achieve the pinning of the d -shell occupancy is the use of an orbital-dependent potential in the framework of the so-called LDA+U method.^{7,8} Speaking about gap values the calculations based on the GW approximation^{9,10} also need to be mentioned, these give *ab initio* gap values which are in good agreement with experiment but do not seem to reproduce the high energy “satellite” in the photoemission spectrum.

In addition to the pinning of the d -shell occupancy, the multiplet structure of the metal ion poses a problem for single-particle theories as well. It is quite well established that the multiplet structure (appropriately modified by the crystal field splitting) of the isolated metal ion persists in the solids. Clear evidence for this point of view comes from the fact that angle integrated valence band photoemission spectra¹¹ as well as x-ray absorption spectra¹² of many transition metal compounds can be reproduced in remarkable detail by configuration interaction calculations solving exactly the problem of a single d -shell hybridizing with a “cage” of ligands. In these calculations it is crucial, however, that the intrashell Coulomb repulsion is treated in full detail. While the cluster method is spectacularly successful for angle-integrated quantities its “impurity” character unfortunately makes it impossible to extract the dispersion relations of \mathbf{k} -resolved single particle excitations.

Actual dispersion relations in the presence of strong Coulomb interaction were first studied by Hubbard,¹³ thereby taking an entirely different point of view as compared to the single-particle picture on which conventional band structure calculations are based. Thereby the d -shells first are considered as isolated, and their affinity and ionization spectra obtained, thereby treating the Coulomb repulsion exactly. In his famous papers Hubbard used a much simplified model, where the orbital degeneracy of the d -level was neglected whence ionization and affinity spectrum of the “half-filled” d -shell collapse to single peak each, with the two peaks separated by the Coulomb energy U . Upon coupling the individual atoms to the solid, the ionization and affinity states of the individual atoms then are systematically broadened to form the two “Hubbard bands.” The coupling to the solid was achieved originally by the famous Hubbard I approximation, but in fact this may be interpreted as a particularly simple form of the cluster perturbation theory (CPT), proposed by Senechal *et al.*,^{14,15} where the individual “clusters” consist of just a single d -shell. This suggests immediately to relax Hubbard’s simplifications and take into account the full complexity of a transition metal oxide including the orbital degeneracy of the d -shell, the full Coulomb interaction between d -electrons in these and the sublattice of ligands. This is essentially the purpose of the present paper.

An important complication is due to the sublattice of ligands. It has been shown by Fujimori and Minami¹¹ that in discarding altogether the sublattice of ligands (in the case of NiO: the oxygen atoms), Hubbard actually went one step too far in his simplification of the model. Namely Fujimori and Minami showed that the top of the valence band in NiO is composed of states, where a hole is predominantly in an oxygen atom, but somehow “associated” with an n -conserving excitation of a neighboring d -shell, i.e., a magnon or a d - d exciton. This type of state might be viewed as a generalization of a Zhang-Rice singlet¹⁶ in the CuO_2 planes of cuprate superconductors. It was then found by Zaanen, Sawatzky, and Allen¹⁷ that there is a crossover between this so-called charge-transfer insulator and a more conventional Mott-Hubbard insulator as a function of two key parameters, the Coulomb repulsion U between electrons in the d -shell and the charge transfer energy Δ , which are defined as

$$E(d^n \rightarrow d^{n+1}\underline{L}) = U - \Delta,$$

$$E(d^n \underline{L} \rightarrow d^{n-1}) = \Delta.$$

Strong experimental support for the picture proposed by Fujimori and Minami is provided by the resonance behavior of the photoemission intensity as seen in photoemission with photon energies near the $2p \rightarrow 3d$ absorption threshold.^{18–20}

Adopting this point of view and using a simplified “Kondo-Heisenberg” model, in which the charge degrees of freedom on Ni were projected out, Bala *et al.*²¹ then obtained dispersion relations of quasiparticles in NiO which in fact do contain the key feature seen in ARPES:^{22,23} the coexistence of strongly dispersive oxygen bands on one hand and a complex of practically dispersionless (i.e., massively renormalized) bands which form the top of the valence band on the other hand.

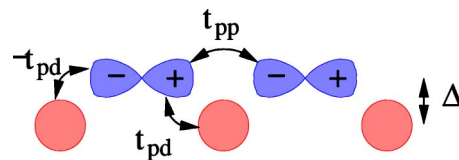


FIG. 1. (Color online) Schematic representation of the Hamiltonian (1) and its parameters.

In the present theory no reduction of the Hamiltonian to a t - J -type model is performed. Rather we use the same basic idea as in the treatment of the Kondo lattice in Ref. 24: the system is divided into subunits which are treated exactly and the hybridization between the subunits is treated approximately. To do so, we define the ground state for vanishing hybridization as the “vacuum state” and treat the charge fluctuations created by the hybridization as “effective Fermions,” for which an approximate Hamiltonian can be derived and solved. It has been shown in Ref. 25 that the Hubbard-I approximation for the single-band Hubbard model can be rederived in this fashion if the subunits are taken to be only a single site—including more complex “composite particles” which extend over several unit cells then improves the agreement with numerical results. The generalized Zhang-Rice singlets discussed above may be viewed as such composite particles. It is shown in Appendix I of Ref. 26 that this treatment is in fact equivalent to the original cluster perturbation theory of Senechal *et al.*^{14,15} provided the subunits into which the system is divided are nonoverlapping. This last requirement poses a substantial problem for transition metal oxides because the rocksalt lattice of NiO cannot be easily divided into nonoverlapping subunits which are still amenable to exact diagonalization without artificially breaking a symmetry of the lattice (which would lead to artificial symmetry breaking in the band structure). We therefore need to adjust the concept of cluster perturbation theory to this situation, which also is an objective of the present work. The remainder of the paper is organized as follows: in Sec. II we discuss a simplified one-dimensional (1D) model, in Sec. III we present the general theory, in Sec. IV we apply the theory to the 1D model and compare the obtained single particle spectra with results from exact diagonalization, in Sec. V we discuss the ARPES spectra of NiO and section VI gives the conclusions.

II. A SIMPLIFIED MODEL

For a start we consider the following minimal version of a 1D charge-transfer model (see Fig. 1):

$$H = -\Delta \sum_{i,\sigma} d_{i,\sigma}^\dagger d_{i,\sigma} + U \sum_i d_{i,\uparrow}^\dagger d_{i,\uparrow} d_{i,\downarrow}^\dagger d_{i,\downarrow} - t_{pd} \sum_{i,\sigma} [d_{i,\sigma}^\dagger (p_{i+1/2,\sigma} - p_{i-1/2,\sigma}) + \text{H. c.}] + t_{pp} \sum_{j,\sigma} (p_{j,\sigma}^\dagger p_{j+1,\sigma} + \text{H. c.}). \quad (1)$$

This model describes a 1D chain consisting of strongly correlated metal(d) orbitals and uncorrelated ligand (p) orbitals.

Henceforth we choose t_{pd} as the unit of energy and unless otherwise stated set $t_{pp}=0$. The relevant filling (which we will consider henceforth) of the model is three electrons (or one hole) per unit cell. While our goal ultimately is to study realistic models for compounds such as NiO, our motivation for studying this highly oversimplified model is as follows: it is simple enough so that reasonably large clusters (up to six unit cells) can be treated by exact diagonalization (ED) and the obtained exact results for the single-particle spectral function then can serve as a benchmark for the analytical theory. The very simple nature of the model thereby is highly desirable because it results in a small number of “bands” so that the comparison with theory is more significant than, e.g., in the case of NiO.

The quantity of main interest is the photoemission and inverse photoemission spectrum, defined as

$$A_d^{(-)}(\mathbf{k}, \omega) = \sum_{\alpha} \sum_{\mu} |\langle \Psi_{\mu}^{(n-1)} | d_{\alpha, \mathbf{k}, \sigma} | \Psi_0^{(n)} \rangle|^2 \times \delta[\omega + (E_{\mu}^{(n-1)} - E_0^{(n)})],$$

$$A_d^{(+)}(\mathbf{k}, \omega) = \sum_{\alpha} \sum_{\nu} |\langle \Psi_{\nu}^{(n+1)} | d_{\alpha, \mathbf{k}, \sigma}^{\dagger} | \Psi_0^{(n)} \rangle|^2 \delta[\omega - (E_{\nu}^{(n+1)} - E_0^{(n)})] \quad (2)$$

where $\alpha \in \{xy, xz, yz, \dots\}$ denotes the type of d -orbital, and $\Psi_{\nu}^{(n)}$ ($E_{\nu}^{(n)}$) denote the ν th eigenstate (eigenenergy) with n electrons, thereby $\nu=0$ corresponds to the ground state. The spectral function for p -electrons is defined in an analogous way.

To get an idea how to construct an adequate theory it is useful to compare the paramagnetic mean-field solution of the model (i.e., with $\Delta \rightarrow \Delta_{MF} = \Delta + \langle n_{\sigma} \rangle U$) and the results of an ED calculation, see Fig. 2. The mean-field solution gives two bands

$$E_{\pm}(k) = \frac{\Delta_{MF}}{2} \pm \sqrt{\left(\frac{\Delta_{MF}}{2}\right)^2 + 4t_{pd} \sin^2\left(\frac{k}{2}\right)}.$$

The lower (fully occupied) one of these has predominant p -character, the upper (half-occupied) one has predominant d -character. In the spectra obtained by exact diagonalization, the p -like bands persist with an almost unchanged dispersion. This is not really surprising, because an electron in the respective state moves predominantly on the p -sublattice and thus will not feel the strong Coulomb interaction on the d -sites very much. The band with predominant d -character, on the other hand, disappears completely in the exact spectra. There is a diffuse band somewhat below $-\Delta = -3t_{pd}$ and a second one at the energy $-\Delta + U = 5t_{pd}$. Clearly, these two resemble the “Hubbard bands” expected for a strongly correlated system and the respective final states have the character of an empty or doubly occupied d -orbital. In addition to these Hubbard bands, however, there is a third group of peaks at energies $\approx +t_{pd}$ which energetically is close to the p -like band, has a mixed p - d character, and which does in fact form the first ionization states of the system. Its closeness to the p -band would seem to suggest that the final states have a hole predominantly on the p -sites, but it also has a

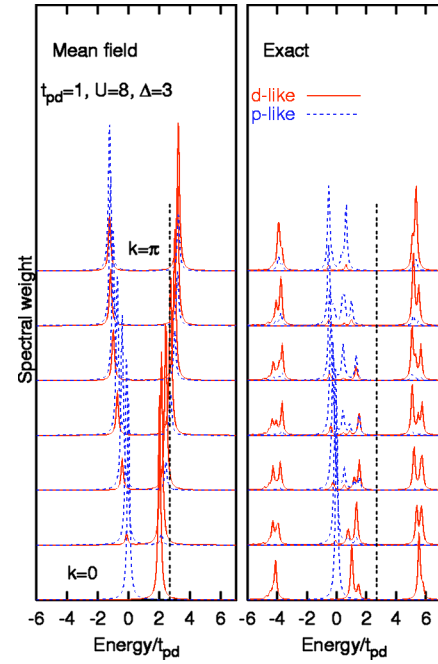


FIG. 2. (Color online) Single particle spectral functions $A^{(-)}(k, \omega)$ and $A^{(+)}(k, \omega)$ obtained by mean-field solution of the model and by exact diagonalization of a system with six unit cells. The wave vector k increases from the lowermost to the uppermost panel in steps of $\frac{\pi}{6}$. δ -functions have been replaced by Lorentzians of width $0.03t_{pd}$. The part to the left (right) of the vertical dashed line shows $A^{(-)}(k, \omega)[A^{(+)}(k, \omega)]$.

significant admixture of d -weight and moreover is closer to the Fermi energy than the p -like band. In the charge transfer system under consideration, the d -like band thus actually splits up into *three* bands, rather than the two Hubbard bands which one might expect.

Despite the highly oversimplified nature of the 1D model, there is actually already a clear analogy to NiO: LDA band-structure calculations²³ produce two well-separated band complexes, the lower one (i.e., the one more distant from the Fermi energy) with predominant oxygen character, the upper one with Ni character. This is quite similar to the mean-field solution in Fig. 2. The actual photoemission spectra, however, show first of all a broad structure at binding energies >8 eV below the top of the valence band. Resonant photoemission experiments^{18,19} show that the final states observed in this energy range have predominantly d^7 character, clearly they should be identified with the d -like band at $-4t_{pd}$ in our model. Next, at binding energies -6 and -4 eV ARPES experiments²³ find a group of strongly dispersive bands which closely resemble the oxygenlike bands obtained from an LDA band structure calculation—they obviously correspond to the dispersive p -like “remnant” of the free-electron band in our model. Finally, the top of the valence band in NiO is formed by a group of almost dispersionless bands, whereby the mixed Ni d^7 and d^8L character of these states is established by resonant photoemission,^{18,19} these states then

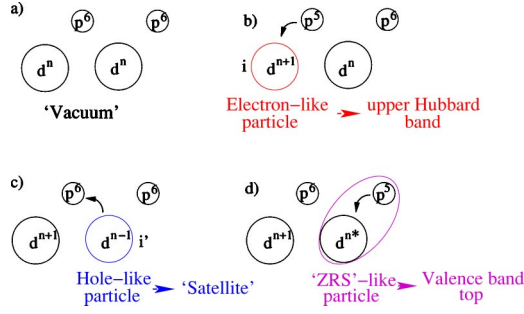


FIG. 3. (Color online) Charge fluctuation processes relative to the purely ionic configuration.

would correspond to the low intensity band which forms the top of the electron annihilation spectrum. The cluster calculation of Fujimori and Minami¹¹ suggests that these states should be viewed as holelike “compound objects” where a hole on oxygen is bound to an excited state of d^8 , a type of state that might be viewed as a generalization of the Zhang-Rice singlet in the CuO_2 planes of cuprate superconductors. As already conjectured by Fujimori and Minami their “compound nature” would make these quasiholes very heavy, which immediately would explain the lack of dispersion seen in the ARPES spectra.²³ Finally, inverse photoemission shows the presence of an upper Hubbard band in NiO which is also present in the spectra of the 1D model.

The above comparison shows that in addition to p -like holes we will need three types of “effective particles” to reproduce the correlated band structure of the model. The two standard Hubbard bands, which correspond to $d^{n\pm 1}$ -like final states are not sufficient here. To get an idea what these states should be, let us start from the ionic limit, $t_{pp}=t_{pd}=0$. The ground state then corresponds to a constant number of electrons, n , in each metal d -shell and completely filled ligand p -shells, see Fig. 3(a). Switching on the hybridization integral t_{pd} then will produce charge fluctuations: in a first step, a hole is transferred into a p orbital, thus producing a d^{n+1} state in d -orbital number i , see Fig. 3(b). The d^{n+1} state has an energy of $U-\Delta$ relative to the original d^n state, and will become our first “effective particle,” these “particles” form the unoccupied Hubbard band. In a second step, the p -like hole can be transferred into a d -orbital $i' \neq i$, thus producing a d^{n-1} state, see Fig. 3(c). The latter has an energy of $+\Delta$ relative to the d^n state and provides the second type of “effective particle,” actually the one that forms the “satellite” in the spectral function. Finally, the hole in i' can be transferred back into a neighboring p -level, thereby leaving the orbital i' in a state d^{n*} , i.e., an eigenstate of d^n other than the original one, see Fig. 3(d). The “compound object” consisting of d^{n*} and a hole in a neighboring p -orbital will be the third type of effective particle, its energy relative to the original d^n state is ≈ 0 , i.e., appropriate to give the top of the valence band. These states might be viewed as generalizations of a Zhang-Rice singlet, or an extreme case of an (either spin- or orbital-like) “Kondo object.” Level repulsion due to hybridization between the d^{n-1} and the d^{n*} states will push the latter up to higher energies relative to the p -like bands, in this way, these states become the first ionization states. In the following, we will try to give the above considerations a

more solid theoretical foundation and apply them to the calculation of “correlated band structures.”

III. GENERAL THEORY

We consider a typical transition metal oxide and restrict our basis to the oxygen $2p$ -orbitals and transition metal d -orbitals. Taking the energy of the p -level as the zero of energy the single-particle terms in the Hamiltonian then take the form

$$H_{pp} = \sum_{i,\kappa,j,\kappa'} \sum_{\sigma} (t_{i,\kappa}^{j,\kappa'} p_{i,\kappa,\sigma}^\dagger p_{j,\kappa',\sigma} + \text{H.c.}),$$

$$H_{pd} = \sum_{i,\alpha,j,\kappa} \sum_{\sigma} (t_{i,\alpha}^{j,\kappa} d_{i,\alpha,\sigma}^\dagger p_{j,\kappa,\sigma} + \text{H.c.}),$$

$$H_{dd} = \sum_{i,\alpha,j,\alpha'} \sum_{\sigma} (t_{i,\alpha}^{j,\alpha'} d_{i,\alpha,\sigma}^\dagger d_{j,\alpha',\sigma} + \text{H.c.}),$$

$$H_d = \sum_{i,\alpha,\beta} \sum_{\sigma} (V_{\alpha,\beta} d_{i,\alpha,\sigma}^\dagger d_{i,\beta,\sigma} + \text{H.c.}), \quad (3)$$

where $d_{i,\alpha,\sigma}^\dagger$ creates a spin- σ electron in the d -orbital $\alpha \in \{xy, xz, yz, \dots\}$ on metal site i and $p_{j,\kappa,\sigma}^\dagger$ creates an electron in the p -orbital $\kappa \in \{x, y, z\}$ on oxygen site j . The $V_{\alpha,\beta}$ combine charge-transfer energy and crystalline electric field. The Coulomb interaction between the d -electrons is

$$H_C = \sum_{\zeta_1, \zeta_2, \zeta_3, \zeta_4} V_{\zeta_1, \zeta_2}^{\zeta_3, \zeta_4} d_{\zeta_1}^\dagger d_{\zeta_2}^\dagger d_{\zeta_3} d_{\zeta_4}, \quad (4)$$

where we have suppressed the site label i , $\zeta = (m, \sigma)$ and $m \in \{-2, \dots, 2\}$ denotes the z -component of the orbital angular momentum. The matrix-elements $V_{\zeta_1, \zeta_2}^{\zeta_3, \zeta_4}$ can be expressed in terms of the three Racah-parameters, A , B , and C .

For a start we take all the hybridization matrix elements t to be zero. In this limit each oxygen is in a $2p^6$ configuration, and each transition metal ion in one of the ground states of $H_{\text{intra}} = H_d + H_C$ with n electrons. In general, this ground state is degenerate, and we deal with this by choosing one of these ground states, which we call $|\Phi_{i,0}\rangle$, for each metal ion. For example, in the case of NiO we would choose the direction of the spin $S=1$ of the d -shell to oscillate between the two sublattices, so as to describe the antiferromagnetic order in the system. We call $|\Phi_{i,0}\rangle$ the corresponding “reference state” on transition metal site i , it obeys $H_{\text{intra}}|\Phi_{i,0}\rangle = E_0^{(n)}|\Phi_{i,0}\rangle$. In the following, we consider the product state of the $|\Phi_{i,0}\rangle$ and the completely filled oxygen- p sublattice as the “vacuum” of our theory. For the 1D model (1) we introduce two d -sublattices A and B and choose

$$|\Phi_{i,0}\rangle = d_{i,\uparrow}^\dagger |0, i\rangle, \quad i \in A;$$

$$|\Phi_{i,0}\rangle = d_{i,\downarrow}^\dagger |0, i\rangle, \quad i \in B;$$

where $|0, i\rangle$ denotes the empty d -orbital i . This choice models the antiferromagnetic spin correlations in the system.

Next, we assume that the hybridization between the sub-systems is switched on. This will create charge fluctuations in the vacuum: in a first step an electron from a p -shell will be transferred into one of the d -orbitals of the neighboring metal ion i , a process frequently denoted as $d^n \rightarrow d^{n+1}\underline{L}$. Due to the many-body character of the Hamiltonian, the resulting state, $d_{i,\alpha,\sigma}^\dagger|\Phi_{i,0}\rangle$, in general is not an eigenstate of H_{intra} , rather, we can express it as a superposition of eigenstates:

$$d_{i,\alpha,\sigma}^\dagger|\Phi_{i,0}\rangle = \sum_{\nu} C_{i,\alpha,\sigma,\nu}|\nu\rangle, \quad (5)$$

where $|\nu\rangle, \nu=0, 1, \dots, \nu_{\text{max}}$ are the eigenstates of the d -shell with $n+1$ electrons. Since we are dealing with a single d -shell these can be obtained by exact diagonalization, which gives us the eigenenergies $E_{\nu}^{(n+1)}$ of the states $|\nu\rangle$ as well as the coefficients $C_{i,\alpha,\sigma,\nu}$. If the $|\nu\rangle$ are chosen to be eigenstates of S_z (as we will assume in all that follows) only a small fraction of the $C_{i,\alpha,\sigma,\nu}$ is different from zero. We now represent the state where the metal ion i is in the state $|\nu\rangle$ by the presence of a “book keeping Fermion,” created by $e_{i,\nu,\sigma}^\dagger$ at the site i . The spin index σ thereby gives the difference in z -spin between the state $|\nu\rangle$ and the reference state $|\Phi_{i,0}\rangle$, in principle this is redundant, but we add it so as to make the analogy with a free-particle Hamiltonian more obvious. An important technical point is that in case the $|\nu\rangle$ are not eigenstates of S_z this labeling is not possible—there may exist states $|\nu\rangle$ which can be reached by transferring an electron of either spin direction into the d -shell i . All in all, the charge fluctuation process then can be described by the Hamiltonian

$$H_1 = \sum_{i,\nu,\sigma} \epsilon_{i,\nu} e_{i,\nu,\sigma}^\dagger e_{i,\nu,\sigma} + \sum_{i,\nu} \sum_{j,\kappa,\sigma} (V_{j,\kappa,\sigma}^{i,\nu} e_{i,\nu,\sigma}^\dagger P_{j,\kappa,\sigma} + \text{H.c.}),$$

$$\epsilon_{i,\nu} = E_{\nu}^{(n+1)} - E_0^{(n)},$$

$$V_{j,\kappa,\sigma}^{i,\nu} = \sum_{\alpha} t_{i,\alpha}^{j,\kappa} \langle \nu | d_{i,\alpha,\sigma}^\dagger | \Phi_{i,0} \rangle = \sum_{\alpha} t_{i,\alpha}^{j,\kappa} C_{i,\alpha,\sigma,\nu}. \quad (6)$$

It is understood that states $|\nu\rangle$ which have $C_{i,\alpha,\sigma,\nu}=0$ for both directions of σ should be omitted from this Hamiltonian. One can see that the “bare” hopping integrals $t_{i,\alpha}^{j,\kappa}$ are multiplied by the coefficients $C_{i,\alpha,\sigma,\nu}$ which have a modulus <1 . The effective Fermions $e_{i,\nu,\sigma}^\dagger$ thus in general have a weaker hybridization with the p -orbitals than the original electrons, which will naturally lead to some kind of “correlation narrowing” of all bands of appreciable d -character.

In the 1D model (1) there is only one state with $n+1$ electrons, namely the state $d_{i\uparrow}^\dagger d_{i\downarrow}^\dagger |0\rangle$. This has an energy of $U-2\Delta$, whence $\epsilon_i = U-\Delta$. For a site i on the A sublattice we thus identify $e_{i\downarrow}^\dagger |vac\rangle = d_{i\downarrow}^\dagger d_{i\uparrow}^\dagger |0\rangle$ and the part H_1 becomes

$$H_1 = (U-\Delta) \sum_{i \in A} e_{i\downarrow}^\dagger e_{i\downarrow} - t_{pd} \sum_{i \in A} [e_{i\downarrow}^\dagger (p_{i+1/2,\downarrow} - p_{i-1/2,\downarrow}) + \text{H.c.}] \quad (7)$$

plus an analogous term which describes the charge fluctuations on the sites of the B -sublattice.

We proceed to the next type of state which is admixed by the hybridization. First, an electron from the metal-ion with $n+1$ electrons may be transferred back to the oxygen atom

with the hole, i.e., $d^{n+1}\underline{L} \rightarrow d^n$. If the metal ion i thereby returns to the reference state $|\Phi_{i,0}\rangle$ this process is described by the term “H.c.” in Eq. (6). If the metal ion returns to an n -electron state $|\lambda\rangle$ other than $|\Phi_{i,0}\rangle$ we should model this by a bosonic excitation $b_{i,\lambda}^\dagger$. Here we will neglect these latter processes—this is presumably the strongest and least justified approximation in the present theory. It implies, for example, that we are neglecting (in the case of NiO) the coupling to $d-d$ excitons and the influence of the quantum spin fluctuations (spin waves) in the 3D $S=1$ Heisenberg antiferromagnet formed by the Ni moments.

A second type of state can be generated by filling the hole in the oxygen shell j with an electron from a d -shell $i' \neq i$, that means $d^n \underline{L} \rightarrow d^{n-1}$. This leaves the d -shell on i' in an eigenstate $|\mu\rangle$ of $n-1$ electrons, the net effect is the transfer of an electron between the d -shells $i' \rightarrow i'$, i.e., precisely the process considered originally by Hubbard. We write

$$d_{i,\alpha,\sigma}|\Phi_{i,0}\rangle = \sum_{\mu} \tilde{C}_{i,\alpha,\sigma,\mu} |\mu\rangle \quad (8)$$

and model the shell i' being in the μ th ionization state by the presence of a holelike book-keeping Fermion, created by $h_{i',\mu,\sigma}^\dagger$. In an analogous way as above we arrive at the following effective Hamiltonian to describe the second type of charge fluctuation:

$$H_2 = \sum_{i,\mu,\sigma} \tilde{\epsilon}_{i,\mu} h_{i,\mu,\sigma}^\dagger h_{i,\mu,\sigma} + \sum_{i,\mu} \sum_{j,\kappa,\sigma} (\tilde{V}_{j,\kappa,\sigma}^{i,\mu} P_{j,\kappa,\sigma}^\dagger h_{i,\mu,\sigma}^\dagger + \text{H.c.}),$$

$$\tilde{\epsilon}_{i,\mu} = E_{\mu}^{(n-1)} - E_0^{(n)},$$

$$\tilde{V}_{j,\kappa,\sigma}^{i,\mu} = \sum_{\alpha} (t_{i,\alpha}^{j,\kappa})^* \langle \mu | d_{i,\alpha,\sigma} | \Phi_{i,0} \rangle = \sum_{\alpha} (t_{i,\alpha}^{j,\kappa})^* \tilde{C}_{i,\alpha,\sigma,\mu}. \quad (9)$$

Since $h_{i,\mu}^\dagger$ creates a holelike particle, the presence of terms like $h_{i\uparrow}^\dagger p_{i\uparrow}^\dagger$ is not unusual—these terms describe particle-hole correlations, not particle-particle correlations as in BCS theory. In the 1D model, the only state with $n-1$ electrons is the empty site $|0\rangle$, which has the energy $E=0$, whence $\tilde{\epsilon} = \Delta$. We identify, for a site i on the B sublattice: $h_{i\uparrow}^\dagger |vac\rangle = |0\rangle$ and the term H_2 reads

$$H_2 = \Delta \sum_{i \in B} h_{i\uparrow}^\dagger h_{i\uparrow} - t_{pd} \sum_{i \in B} [(p_{i+1/2,\downarrow}^\dagger - p_{i-1/2,\downarrow}^\dagger) h_{i\uparrow}^\dagger + \text{H.c.}] \quad (10)$$

plus an analogous term describing the A sublattice.

As already stated, the second type of charge transfer excitation describes the transfer of an electron between two d -shells via an intermediate state with a hole in an oxygen p -shell. If there are direct $d-d$ transfer integrals, this process can also occur in one step. The respective part of the effective Hamiltonian can be constructed in an entirely analogous fashion as the parts above, since it is lengthy, we do not write it down in detail.

We proceed to the last type of “effective particle” that we

will consider. If the d -shell on atom i is in an eigenstate of $n-1$ electrons (which would be described by the $h_{i,\mu}^\dagger$ -particle) it is possible that an electron from a neighboring p -shell is transferred to the d -shell, thereby leaving the d -shell i in an eigenstate $|\lambda\rangle$ of n electrons other than the reference state $|\Phi_{i,0}\rangle$. We will consider the ‘‘compound object’’ consisting of the ‘‘excited’’ d^n state $|\lambda\rangle$ on site i and a hole in a linear combination $\psi_{\alpha,\sigma}^\dagger$ of p -orbitals on the nearest neighbors of i as a further effective particle, created by $z_{i,\lambda,\alpha,\sigma}^\dagger$. Here $\alpha \in \{xy, xz, yz, \dots\}$ denotes the symmetry of the linear combination of p -orbitals, which is such as to hybridize with exactly one of the $d_{i,\alpha,\sigma}^\dagger$ on site i . For an ideal tetrahedral cage of oxygen atoms around each metal ion there is exactly one combination $\psi_{\alpha,\sigma}^\dagger$ for each α . The creation and annihilation of the z -particles can be described by the term

$$H_3 = \sum_{i,\lambda,\alpha,\sigma} \epsilon_{i,\lambda,\alpha} z_{i,\lambda,\alpha,\sigma}^\dagger z_{i,\lambda,\alpha,\sigma} + \sum_{i,\mu,\lambda,\alpha} (V_{i,\lambda,\alpha,\sigma}^\mu z_{i,\lambda,\alpha,\sigma}^\dagger h_{i,\mu,\sigma} + \text{H.c.}),$$

$$\epsilon_{i,\lambda,\alpha} = E_\lambda^{(n)} - E_0^{(n)} - \zeta_\alpha,$$

$$V_{i,\lambda,\alpha,\sigma}^\mu = -T_\alpha \langle \lambda | d_{\alpha,\sigma}^\dagger | \mu \rangle. \quad (11)$$

Here $\zeta_\alpha = \langle 0 | \psi_{\alpha,\sigma} [H_{pp}, \psi_{\alpha,\sigma}^\dagger] | 0 \rangle$ denotes the kinetic energy of the combination $\psi_{\alpha,\sigma}^\dagger$, it can be expressed in terms of the integrals $(pp\sigma)$ and $(pp\pi)$. Also, $T_\alpha = \langle 0 | d_{i,\alpha,\sigma} [H_{pd}, \psi_{i,\alpha,\sigma}^\dagger] | 0 \rangle$ is the hybridization matrix element between $\psi_{\alpha,\sigma}^\dagger$ and $d_{i,\alpha,\sigma}^\dagger$ and can be written in terms of $(pd\sigma)$ and $(pd\pi)$.

In the 1D model, the only ‘‘excited’’ state on the A sublattice is the state $d_{i,\downarrow}^\dagger | 0 \rangle$. The only possible combination of p orbitals which hybridizes with a d -orbital is $\psi_{i,1,\sigma}^\dagger = 1/\sqrt{2}(p_{i+1/2,\sigma}^\dagger - p_{i-1/2,\sigma}^\dagger)$, which has $\zeta_1 = -t_{pp}$. There is therefore just one z^\dagger -like particle on the A -sublattice, which corresponds to site i being in the state $d_{i,\downarrow}^\dagger | 0 \rangle$ and having an extra hole in the combination $\psi_{i,1,\sigma}^\dagger$. The total energy is $E = -\Delta + t_{pp}$ whence $\epsilon = t_{pp}$ and the corresponding Hamiltonian reads

$$H_3 = t_{pp} \sum_{i \in A} z_{i\uparrow}^\dagger z_{i\uparrow} - \sqrt{2} t_{pd} \sum_{i \in A} (z_{i\uparrow}^\dagger h_{i\uparrow} + \text{H.c.}) \quad (12)$$

and, again, a corresponding term for the B -sublattice. This concludes the types of state which we take into account. We are thus assuming that the hole always is on a nearest neighbor of the d^m state, this means that we truncate the ‘‘Kondo cloud’’ which is not exactly true. In principle this approximation could be relaxed by including more complex composite particles but here we do not include these.

In order for the mapping between the actual system and the ‘‘book-keeping Fermions’’ to be a faithful one, we must require that the occupation of any d -site is either 0 or 1, otherwise, the state of the respective d -shell is not unique. This implies that the book-keeping Fermions e^\dagger , h^\dagger , and z^\dagger have to obey a hard-core constraint, in exactly the same way as, e.g., the magnons in spin-wave theory for the Heisenberg antiferromagnet (HAF). It is well known, however, that linear spin-wave theory for the HAF, which neglects this hard-core constraint altogether and treats the magnons as free Bosons, gives an excellent description of the antiferromag-

netic phase, even in the case of $S=1/2$ and $d=2$, where quantum fluctuations are strong. The reason is that the density n of magnons/site obtained self-consistently from linear spin wave theory is still relatively small, whence the probability that two magnons occupy the same site and thus violate the constraint is $\propto n^2 \ll 1$. For the same reason we expect that relaxing the constraint in the present case and treating the book-keeping Fermions as free Fermions will be a very good approximation, its physical content is the assumption that the probability of charge fluctuations is small, which is certainly justified in a Mott- or charge-transfer-insulator. For completeness we note that there is also a certain interference between the z^\dagger particle and the holes on oxygen in the sense that the respective creation and annihilation operators do not exactly anticommute. Again, we neglect this, with the justification again being the very low density of the z^\dagger and p^\dagger particles.

Adding the various terms in the Hamiltonian and the direct p - p hopping H_{pp} we obtain a Hamiltonian which describes the lowest order charge fluctuation processes while still being readily solvable by Fourier and Bogoliubov transform with the result:

$$H = \sum_{\mathbf{k}, \zeta, \sigma} E_{\mathbf{k}, \zeta, \sigma} \gamma_{\mathbf{k}, \zeta, \sigma}^\dagger \gamma_{\mathbf{k}, \zeta, \sigma}, \quad (13)$$

where ζ is a band index. Quantities of physical interest now can be readily calculated. Let us first discuss the electron count. We assume that the reference states for the d -shell have n electrons each. Then, the total number of electrons/unit cell is $n_e = n \cdot n_d + 6 \cdot n_o$ where $n_d(n_o)$ denote the number of metal (oxygen) atoms in the unit cell. On the other hand we have

$$n_e = n \cdot n_d + \frac{1}{N} \sum_{\mathbf{k}, \sigma} \left(\sum_{j, \kappa} P_{\mathbf{k}, j, \kappa, \sigma}^\dagger P_{\mathbf{k}, j, \kappa, \sigma} + \sum_{i, \mu} e_{\mathbf{k}, i, \mu, \sigma}^\dagger e_{\mathbf{k}, i, \mu, \sigma} - \sum_{i, \nu} h_{\mathbf{k}, i, \nu, \sigma}^\dagger h_{\mathbf{k}, i, \nu, \sigma} - \sum_{i, \alpha, \lambda} z_{\mathbf{k}, i, \alpha, \lambda}^\dagger z_{\mathbf{k}, i, \alpha, \lambda, \sigma} \right). \quad (14)$$

Here the sums over j and i run over the p - and d -shells in one unit cell and the equation follows readily from the electron/hole-like character of the various effective Fermions. This can be rewritten as

$$n_e = n \cdot n_d + \frac{1}{N} \sum_{\mathbf{k}, \zeta, \sigma} \gamma_{\mathbf{k}, \zeta, \sigma}^\dagger \gamma_{\mathbf{k}, \zeta, \sigma} - \sum_{\sigma} (\mu_{\text{tot}, \sigma} + \lambda_{\text{tot}, \sigma}); \quad (15)$$

where $\mu_{\text{tot}, \sigma}$ denotes the total number of ionization states in the unit cell which can be reached by extracting a spin σ electron from one of the $|\Phi_{i,0}\rangle$, and $\lambda_{\text{tot}, \sigma}$ the total number of z^\dagger -particles in the unit cell which couple to one of these ionization states. If we assume that the band structure is spin independent (which is the case for NiO) these numbers must be independent of σ and we obtain the following requirement for the electron number:

$$\sum_{\mathbf{k},\sigma} \gamma_{\mathbf{k},\alpha,\sigma}^\dagger \gamma_{\mathbf{k},\alpha,\sigma} = N[6n_o + 2(\mu_{tot} + \lambda_{tot})]. \quad (16)$$

The number of occupied bands in the system thus is $n_{occ} = 3n_o + \mu_{tot} + \lambda_{tot}$. Since the total number of bands produced by our formalism is $3n_o + \nu_{tot} + \mu_{tot} + \lambda_{tot}$, we find that the chemical potential falls exactly into the gap between the $3n_o + \mu_{tot} + \lambda_{tot}$ bands which correspond (in the limit of vanishing hybridization) to the oxygen $2p$ states, the ionization states of the d -shell and the $d^8\bar{L}$ -type states on one hand and the ν_{tot} bands, which correspond to the affinity states of the d -shells on the other hand. Obviously, this is the physically correct position of the chemical potential.

The quantity of main interest to us, the single-particle spectral function $A_\alpha(\mathbf{k}, \omega)$ can be obtained from the eigenvectors of the Hamilton matrix once the resolution of the d -electron creation/annihilation operator is known. Were it not for the presence of the z^\dagger -like particles, we could write

$$d_{\mathbf{k},\alpha,\sigma}^\dagger = \sum_{\nu} C_{i,\alpha,\sigma,\mu} e_{\mathbf{k},\mu,\sigma}^\dagger + \sum_{\nu} \tilde{C}_{i,\alpha,\sigma,\nu}^* h_{-\mathbf{k},\nu,\bar{\sigma}}, \quad (17)$$

which is easily verified by taking matrix-elements between the right- and left-hand side. However, the presence of the z^\dagger -like ‘‘particle’’ complicates this. Due to their ‘‘compound nature’’ the processes by which the electron annihilation operator couples to a z^\dagger -particle are rather complicated. For example, one might envisage a process in which an electron in a d^{n+1} configuration on site i is annihilated, leaving the d -shell in a d^{n*} state (i.e., an eigenstate of d^n other than the reference state $|\Phi_{i,0}\rangle$ on site i). Then, if simultaneously a hole happens to be present in a p -orbital next to site i , this process would create a z^\dagger -like particle on site i , leading to an operator product of the type $z_i^\dagger h_i \psi_{i\alpha}$ to describe this process. Similarly, if a d^{n*} state is somehow created on a site i (this is not possible in the framework of the Hamiltonian which we wrote down above—it would necessitate terms including the bosonic excitations $b_{i,\lambda}^\dagger$ discussed above) and a hole is created in a p -orbital next to this site, this would result in the creation of a z^\dagger -like particle on site i . This process could be described by a product of the type $z_i^\dagger \psi_{i\alpha} b_i$. Due to the fact that these processes all involve products of three operators one might expect that they lead predominantly to an incoherent continuum in the spectral function. All in all, we may thus expect that this type of process will not contribute substantially to the photoemission intensity for the dominant peaks. Clearly, the problem in calculating the spectral weight is a drawback of the theory—it should be noted, however, that there is a very clear physical reason for this problem, namely the ‘‘compound nature’’ of the z_i^\dagger particles and this should be reflected in any theoretical description.

Finally we comment on the relationship with the CPT proposed by Senechal *et al.*^{14,15} Following Appendix I of Ref. 26 it can be shown that the present theory is equivalent to CPT provided the z^\dagger particles are omitted. Each d -shell thereby would form a ‘‘cluster’’ of its own whereas the ligand sublattice as a whole forms one additional cluster. This ‘‘ligand cluster’’ therefore has an infinite size but this is irrelevant for CPT because being a noninteracting system its Green’s functions still can be calculated exactly. An obvious

advantage of our subdivision is that there is no supercell structure and hence no artificial gaps in the band structure. One might worry that the size of the ‘‘clusters’’ is too small, however, in Ref. 24 it was shown for the periodic Anderson model that clusters comprising only a single unit cell give quite satisfactory results for the quasiparticle dispersion. In the next section this will be seen to be true also for the charge transfer model (1). In Ref. 15 Senechal *et al.* treated a two-band model for CuO_2 planes of cuprate superconductors by CPT thereby coupling clusters of size 2×2 unit cells with three orbitals/unit cell, in the present case, however, no cluster comprising more than one d -shell can be treated by exact diagonalization because of the prohibitively large dimension of the Hilbert space.

A highly desirable approach would be to couple via CPT clusters of the type used by Fujimori and Minami¹¹—that means a single d -shell together with the octahedron formed by its six nearest oxygen neighbors. Unfortunately any two of these octahedra centered on neighboring Ni sites share one oxygen atom—this approach would therefore necessitate a version of CPT which uses site-sharing clusters. At present, it is unclear if it is possible to construct such a theory.

IV. COMPARISON WITH EXACT DIAGONALIZATION

Our theory involves a number of strong approximations which need to be checked in some way. Here we present a comparison of results obtained for the 1D model (1) and exact diagonalization of finite clusters. For the 1D model, systems with six unit cells easily can be solved exactly on a computer and we use these results as a benchmark to check our theory. The simplicity of the model actually makes the comparison more significant than, e.g., in the case of a realistic model for NiO because we expect only a small number of ‘‘bands’’ whence any disagreement will be more obvious.

Before we discuss results for physical quantities let us address one of the key approximations of our theory, namely the neglect of the hard-core constraint which in principle should be obeyed by the book-keeping Fermions. Solving the 1D model with $\Delta=3$, $U=6$ gives the GS expectation values $\langle e_i^\dagger e_i \rangle = 0.151$, $\langle h_i^\dagger h_i \rangle = 0.004$, and $\langle z_i^\dagger z_i \rangle = 0.0007$. This implies that the probability for a violation of the constraint on any given d -site is ≈ 0.03 , i.e., entirely negligible. Simply relaxing the constraint thus is probably an excellent approximation.

Next, Fig. 4 compares the total energy/site and the d -occupancy, which is a measure for the charge-transfer form $p \rightarrow d$, as obtained by exact diagonalization and from the theory. Obviously, there is good agreement. Fig. 5 shows a comparison between the single particle spectral function obtained from the theory and by exact diagonalization of a system with six unit cells. To obtain a denser mesh of k -points, spectra for a system with periodic and antiperiodic boundary conditions have been used for the exact diagonalization part, that means $k=0, \pi/3, 2\pi/3$, and π have been calculated with PBC, the ones for $k=\pi/6, \pi/2$, and $5\pi/6$ have been obtained with ABC. Although there is no rigorous proof for this, experience shows that combining spectra with PBC and ABC gives quite ‘‘smooth’’ dispersion relations, as

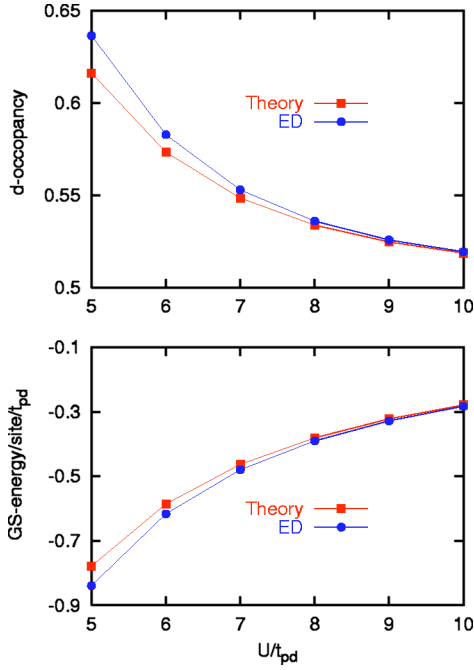


FIG. 4. (Color online) Ground state energy and d -occupation as a function of U for $\Delta=3$, $t_{pd}=1$ as obtained by exact diagonalization of a system with six unit cells and from the present theory. The trivial contribution of $-\Delta$ has been subtracted off from the ground state energy.

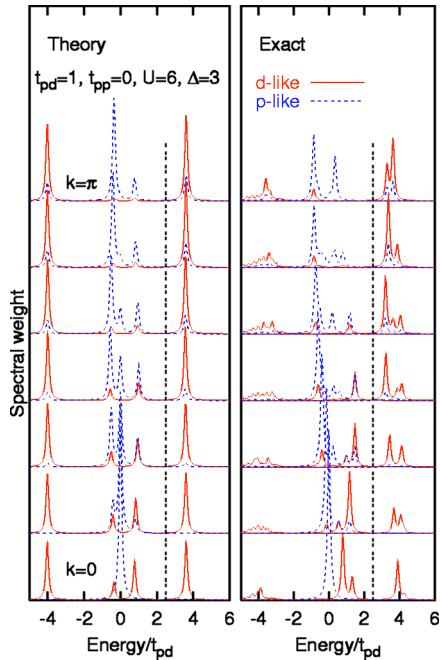


FIG. 5. (Color online) Single particle spectral functions $A^{(-)}(k, \omega)$ and $A^{(+)}(k, \omega)$ obtained by the present theory and by exact diagonalization of a system with six unit cells. The wave vector k increases from the lowermost to the uppermost panel in steps of $\pi/6$, to that end the figure combines spectra obtained with periodic and antiperiodic boundary conditions. The part to the left (right) of the vertical dashed line shows $A^{(-)}(k, \omega)$ [$A^{(+)}(k, \omega)$].

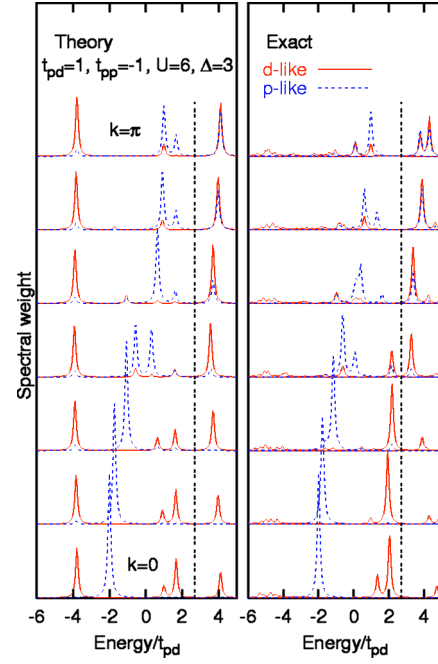


FIG. 6. (Color online) Same as Fig. 5 but with different parameter values.

can also be seen in the present case. In order to suppress the Luttinger-liquid behavior expected for 1D systems, a staggered magnetic field of $0.1t_{pd}$ was applied. The agreement between theory and exact diagonalization then is obviously quite good. The dispersion and spectral character of the main “bands” in the numerical spectra is reproduced quite well. The main difference concerns the very strong damping of the lower Hubbard band at $E \approx -4t_{pd}$, which actually forms a broad continuum rather than a well-defined band in the numerical spectra. Moreover, the upper Hubbard band at $E \approx 4t_{pd}$ has some “fine structure” in the numerical spectra, which is not reproduced by the theory. On the other hand, our theory does not include any damping mechanism such as the coupling to spin excitations, so one cannot expect it to reproduce such details. Another slight discrepancy concerns the bandwidth of the oxygen band at $E \approx 0$, which is somewhat underestimated by theory. Apart from that and a few low-intensity peaks in the numerical spectra, however, there is a rather obvious one-to-one correspondence between the bands in the theoretical spectra and the exact ones. Next, we consider the spectra for a nonvanishing p - p hopping, $t_{pp} = -1$, see Fig. 6. Again, there is good agreement between theory and numerics, with the main discrepancy being again the damping of the satellite and the fine structure of the upper Hubbard band. Still, there is a clear one-to-one correspondence between theory and exact spectra. An interesting check is provided by inverting the sign of t_{pp} . One might expect at first sight that the only effect is to invert the dispersion of the p -like band. Inspection of the Hamiltonian (12) shows, however, that inverting the sign of t_{pp} also affects the energy of the z^\dagger -particle, and hence should lead to a shift of the corresponding band. The actual spectra in Fig. 7 then show that this is indeed the case in the numerical spectra. The z -like band is shifted to higher energies by very

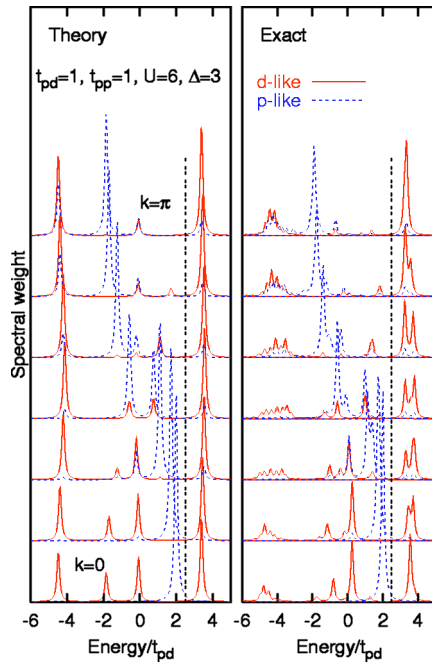


FIG. 7. (Color online) Same as Fig. 5 but with different parameter values.

nearly the amount of $2t_{pd}$ expected from theory, so that the lowest hole-addition states now belong to the p -like band. The fact that the inversion of the sign of t_{pp} has precisely the effect predicted by theory is a strong indication that this is indeed the correct interpretation of the low energy peaks in the spectra.

V. THE BAND STRUCTURE OF NiO

Summarizing the results of the preceding section we may say that the theory reproduces the numerical spectra and the trends under a change of parameters remarkably well, an indication that despite its simplicity the theory really captures the essential physics of the two-band model. This is encouraging to apply it to a real material, NiO. In applying the above procedure to NiO we first performed a standard LDA band-structure calculation in the framework of the LMTO-method²⁷ for NiO (thereby assuming a paramagnetic ground state) and obtained the LCAO parameters by a fit. For simplicity no overlap integrals were taken into account. A comparison between the LDA band structure and the LCAO fit is shown in Fig. 8 (the LDA result is essentially identical to that of Ref. 23), the hybridization integrals and site energies obtained by the fit are given in Table I. We have also obtained LCAO parameters for an antiferromagnetic LSDA band structure, and those parameters which can be compared (such as the hybridization integrals) do not differ significantly. All in all this procedure gives quite reliable estimates for the values of the various hopping integrals. The LDA band structure broadly can be divided into two complexes of bands: the lower one at energies between -8 and -3 eV has almost pure oxygen p -character. In other words, a hole in this band would move almost exclusively on the oxy-

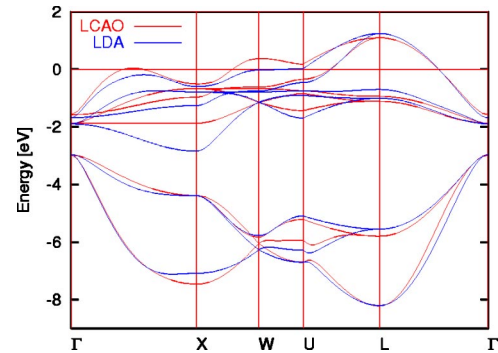


FIG. 8. (Color online) LDA band structure for paramagnetic NiO and LCAO fit. The Fermi energy is taken to be zero.

gen sublattice and have only a very small probability to be on a Ni ion. One may thus expect that these states persist essentially unchanged in the correlated ground state. Next, the complex between -3 and $+1$ eV has almost exclusively Ni $3d$ character. The LDA band structure thus would seem to suggest that there are states where a hole is moving essentially from one Ni site to another, which have a less negative binding energy, i.e., which are closer to the Fermi energy, i.e., which are closer to the Fermi energy than the states where the hole is moving in the oxygen sublattice. Clearly, in view of the value of the charge transfer energy $\Delta > 0$, which is consistently suggested by a variety of methods,^{4,11,12} this is a quite wrong picture of the electronic structure. Next, we consider the Racah parameters B and C . These differ only slightly from their values for free ions and we took the values from Fujimori and Minami¹¹ $B = 0.127$ eV, $C = 0.601$ eV for d^8 and $B = 0.138$ eV, $C = 0.676$ eV for d^9 . In general, these parameters are screened by covalency between d -orbitals and ligands²⁸ but for simplicity we keep the “bare” values.

This leaves us with two parameters, which require a special treatment, namely the Racah parameter A , which is subject to substantial solid-state screening, and the difference of site energies between the Ni $3d$ -level and the oxygen $2p$ -level. The Racah parameter A is related to the Coulomb energy U , which can be obtained from “pure d -quantities” according to $U = E_0^{n+1} + E_0^{n-1} - 2E_0^n$. Here we used the values $U = 8.7$ eV and $\Delta = 1.5$ eV. Similar values for U have been obtained by Fujimori and Minami¹¹ from a cluster fit of the

TABLE I. Hybridization integrals and site-energies (in eV) obtained by a LCAO fit to the paramagnetic LDA band structure of NiO.

| | Ni-O | O-O | Ni-Ni | ϵ |
|--------------|--------|--------|--------|-------------------------|
| $(s\sigma)$ | | 0.023 | | |
| $(sp\sigma)$ | | | | $\epsilon_{2s} = -10$ |
| $(pp\sigma)$ | | 0.665 | | |
| $(pp\pi)$ | | -0.104 | | $\epsilon_{2p} = -4.8$ |
| $(sd\sigma)$ | -0.720 | | | |
| $(pd\sigma)$ | -1.310 | | | $\epsilon_{3d} = -1.13$ |
| $(pd\pi)$ | 0.382 | | | |
| $(d\sigma)$ | | | -0.201 | |

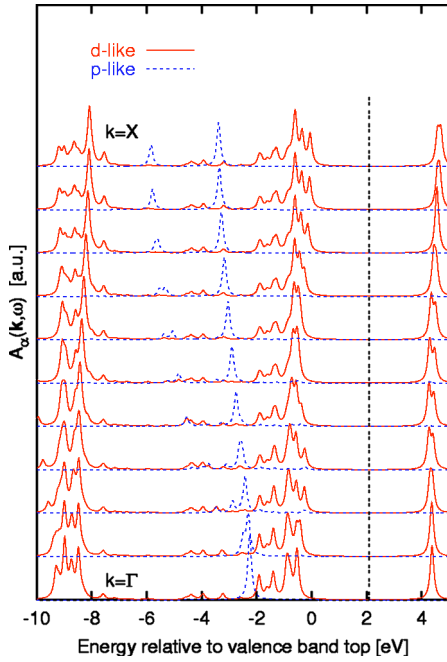


FIG. 9. (Color online) Single particle spectral densities [see Eq. (2) for a definition] for antiferromagnetic NiO obtained by the present theory. The momenta are along the (100) direction, the top of the valence band is the zero of energy. δ -functions are replaced by Lorentzians of width 0.075 eV, the d -like spectral density is multiplied by a factor of 4.

valence band photoemission spectrum, by van Elp *et al.*¹² from a cluster fit to the x-ray absorption spectrum and by Norman and Freeman⁴ from density functional calculations. The value of Δ is somewhat small compared to others, which are around 2.5 eV.

Then, the problem of a single d -shell was solved by exact diagonalization in the 7, 8, and 9 electron subspaces. The maximum dimension of the Hilbert space was 120 for $n=7$. A nonvanishing CEF parameter $10Dq=0.05$ eV was applied in order to stabilize the correct $t_{2g}^6 e_g^2 A_{2g}$ ground state for d^8 in O_h -symmetry. To account for the antiferromagnetic nature of the GS of NiO, we chose the reference state $|\Phi_{i,0}\rangle$ to be the $S_z=1$ member of the ${}^3A_{2g}$ multiplet on the Ni-sites of one sublattice, and the $S_z=-1$ member on the other one. Since we neglect spin-orbit coupling the direction of the spin quantization axis is arbitrary and has no influence on the spectral function. The kinetic energies of the t_{2g} and e_g -like combinations of p -orbitals, which enter the energy of the z -like particles, are $\epsilon_{t_{2g}}=(pp\sigma)-(pp\pi)$ and $\epsilon_e=(pp\pi)-(pp\sigma)$, the respective hybridization integrals are $T_{t_{2g}}=2(pd\pi)$ and $T_e=\sqrt{3}(pd\sigma)$. All in all, the rank of the effective Hamilton matrix to be diagonalized was ≈ 250 , i.e., quite moderate. To improve the agreement with experiment, the following minor adjustments of parameters were made: the $p-p$ hybridization integrals were reduced by a factor of 0.8, and the $d-p$ hybridization integrals were increased by a factor of 1.1.

The full single-particle spectral functions obtained along the (100) direction for antiferromagnetic NiO then is shown in Fig. 9 It differs quite significantly from what one would expect on the basis of the LDA band structure (see Fig. 8)

but instead shows the same overall structure as in the 1D model, compare to Fig. 2. As was the case for the 1D model one can broadly speaking distinguish four complexes of bands. At binding energies < -8 eV, there is a broad continuum of bands with strong d -weight. Analysis of the wave functions shows that the respective states have (mainly) h^\dagger (i.e., d^7) character, with some admixture of z^\dagger (i.e., $d^8\bar{L}$) and (less) admixture of O2p character. Clearly these bands should be identified with the “satellite” in the experimental NiO spectra. By analogy with the 1D model we may expect that these high energy states undergo substantial broadening as is indeed seen in experiment. In Fig. 9 the satellite by and large disperses upwards as one goes away from Γ —Shen *et al.*²³ interpreted their data as showing a downward dispersion of the satellite. On the other hand this feature is rather broad and composed of many “subpeaks” so that it may be difficult to make really conclusive statements about the dispersion of the spectral weight without a full calculation of the spectral weight, including the “radiation characteristics” of the individual d -orbitals, final states effects, etc.

Next, there is a group of strongly dispersive bands of predominant O2p character, which closely resembles the lower complex of bands in the LDA calculation, see Fig. 8. In view of their almost pure oxygen character it is no surprise that these bands are hardly influenced by whatever happens on the Ni sites. Next comes a group of practically dispersionless bands which form the top of the valence band. They have mainly z^\dagger (i.e., $d^8\bar{L}$) character with some admixture of h^\dagger (i.e., d^7). Due to their strong z^\dagger -character these bands probably are influenced most strongly by our approximation to omit any terms involving z^\dagger -operators in the spectral weight operator (17). We may expect that taking the processes discussed there will probably enhance the weight of these states and also add some more p -like weight to these peaks.

The topmost peak is rather intense and actually composed of several “subpeaks”—it is in fact the only feature in this energy range which shows significant dispersion. Below this broad peak, there are several bands with lower intensity and practically no dispersion—all of this exactly as seen in the ARPES experiment by Shen *et al.*²³ Figure 10 shows a more detailed comparison of the dispersion of “significant peaks” in the photoemission part of the theoretical spectra with the experimental peak dispersions as reported by Shen *et al.* It can be seen that the agreement is quite good. Along both (100) and (110) the main discrepancy is the position of bands C and D [or D_1 along (110)] which are somewhat higher in energy in the theory, still, the discrepancy is only 0.7 eV. In view of the fact that we have used the simplest set of parameters this is quite good agreement. The band portion Ea which is unusual due to its downward curvature has actually been observed by Shen *et al.* in normal emission (see Fig. 6 of Ref. 23). The part Eb seems to correspond to the experimental band E itself—it has rather low spectral weight for momenta close to Γ .

Finally, Fig. 11 gives the dispersion of the “sub-bands” of the broad structure A at the valence band edge. This fine structure has not been resolved experimentally as yet, however, Shen *et al.* found evidence for at least three “subpeaks” and also for a quite substantial dispersion, although this

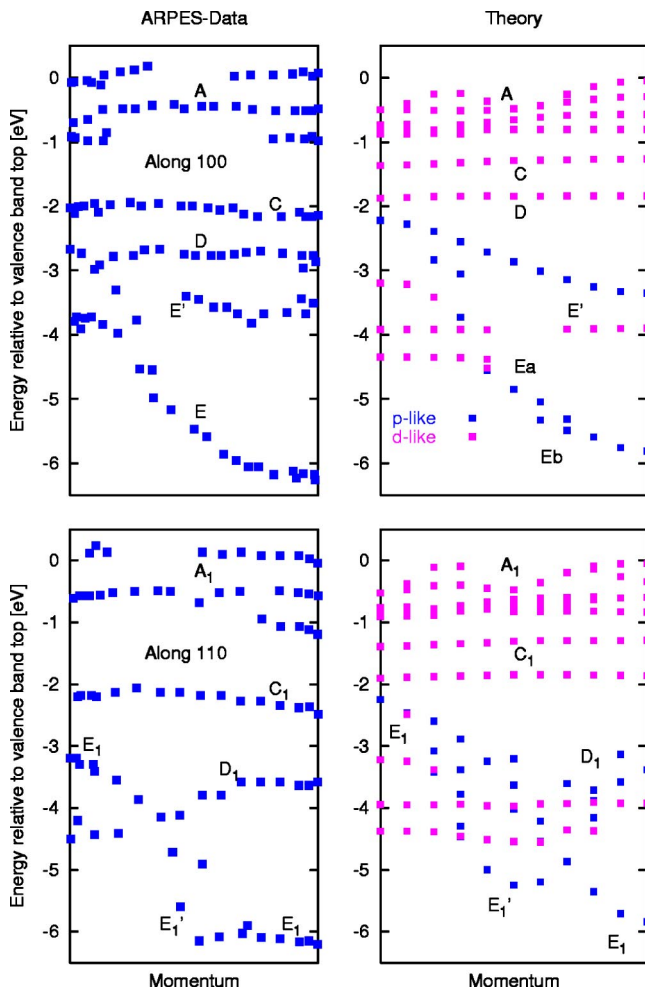


FIG. 10. (Color online) Comparison between the experimental peak dispersions determined by ARPES in non-normal emission (taken from Fig. 12 of Ref. 23) and the position of “significant peaks” in the theoretical spectra. The labels on the “bands” indicate a possible correspondence between experiment and theory.

made itself felt only as a dispersion of the line shape of the broad peak. Looking at Fig. 9 and 10 of Ref. 23 it would appear that along (100) there is an overall “upward” dispersion of the topmost peak A as one moves from $\Gamma \rightarrow X$ with two local maxima of the upper edge of A just after Γ and just before X with the whole band complex being most narrow approximately halfway between Γ and X. It can be seen already from Fig. 10 that this dispersion of the peak-shape of A is reproduced quite well by theory. Similarly, along (110) the broad band complex seems to have its minimum width halfway between Γ and X. At least these qualitative results are quite consistent with the dispersion in Fig. 11. Clearly a more detailed study of the fine structure of feature A would provide an interesting check of the present and other theories for the band structure of NiO. Another stringent check for theory would be to unravel the orbital character of the individual flat bands such as C and D by studying their intensity as a function of photon polarization and energy.

Finally, we mention the upper Hubbard band, with the corresponding final states having predominantly e^{\uparrow} -character. The insulating gap has a magnitude of 4.3 eV, which is consistent with experiment.³ Figure 12 shows the angle integrated (i.e., \mathbf{k} -integrated) photoemission and inverse photoemission spectrum. By and large there is reasonable agreement with experiment. The fact that theory puts the dispersionless bands C and D too close to the top of the valence bands leads to a too weak shoulder on the negative binding energy side of the “main peak” at the top of the valence bands.

VI. CONCLUSION

In summary, we have presented a theory for the single-particle excitations of charge-transfer insulators. The basic idea is to interpret the charge fluctuations out of the purely ionic configuration as “effective Fermions” and derive and solve an effective Hamiltonian for these. This is the same physical idea which is underlying both the Hubbard I ap-

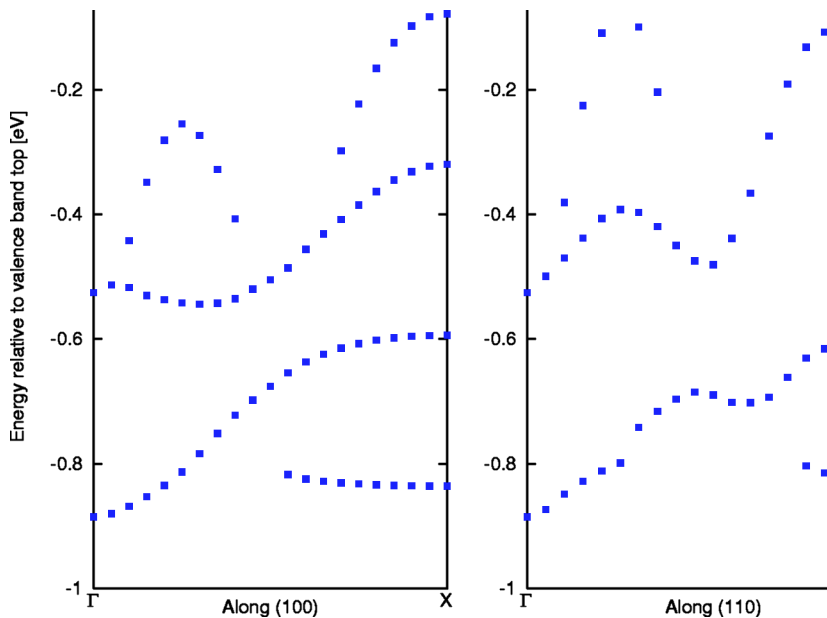


FIG. 11. (Color online) Fine structure of the broad peak which forms the top of the valence band structure in antiferromagnetic NiO. The symbols give the positions of peaks with appreciable weight.

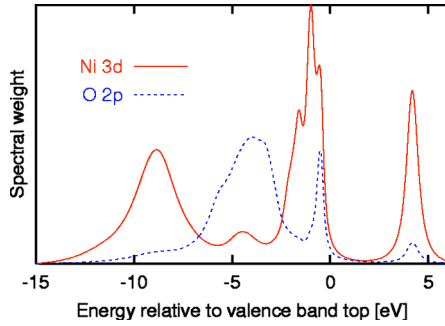


FIG. 12. (Color online) Momentum integrated spectral weight for antiferromagnetic NiO. To simulate a photoemission spectrum the Lorentzian broadening has been taken energy dependent according to $\delta = 0.4 \text{ eV} + (\omega - 1 \text{ eV}) \cdot 0.1$.

proximation and the cluster perturbation theory and, as demonstrated above, when applied to a realistic model of a charge-transfer insulator these methods, which so far have been restricted to more “model-type” systems, give indeed quite satisfactory agreement with experiment. The key approximation, namely to treat the Hubbard-like operators describing the charge fluctuations as free Fermions, thereby is well justified because of the low density of these effective Fermions, which renders their (strong) interaction largely irrelevant. A systematical way to relax this approximation would be the T -matrix approach, as demonstrated by Kotov *et al.*²⁹ It should be noted that the calculation is computationally no more demanding than a conventional band-structure calculation and can be “automated” almost completely. The weakest link in the chain thereby is the necessity to perform an LCAO-fit to an LDA band structure.

One important conceptual problem is the necessity to break the symmetry which originates from the degeneracy of the ground state multiplet of a single transition metal ion and choose the “reference states” $|\Phi_{i,0}\rangle$ “by hand.” However, one might as well consider choosing an *ansatz* for these reference states which takes the form of a linear combination $|\Phi_{i,0}\rangle = \sum_{\nu} \alpha_{i\nu} |\nu\rangle$, where the sum extends over the GS multiplet, and determine the coefficients $\alpha_{i\nu}$ from the requirement of minimum total energy. In this way spin and orbital ordering could be studied in much the same way as lattice parameters are optimized in conventional LDA calculations and since all “ingredients” for the Goodenough-Kanamori rules³⁰ are taken into account, this may be a quite promising method. Since spin-orbit coupling also can be trivially included in the exact diagonalization of the isolated d -shells one might even hope to address magnetic anisotropies and/or anisotropic exchange interactions. A procedure for the improvement of CPT calculations on model Hamiltonians which is similar in spirit has been proposed by Potthoff *et al.*³¹

One major drawback of the theory clearly is the approximate nature of the calculation of the spectral weight. It should be noted, however, that there is a very clear physical reason for this problem, namely the “compound nature” of the ZRS-like states which form the top of the valence band. If the present interpretation of these states is the correct one, basically any theory will face similar problems. One possible way out would be to derive a version of the original CPT which can work with site-sharing clusters.

Finally, we would like to discuss the relationship between our theory and previous workers in the field. Manghi *et al.*³² and Takahashi and Igarashi³³ have calculated the quasiparticle band structure of NiO more along the lines of conventional many-body theory. Starting from a paramagnetic LDA band structure (Ref. 32) or an antiferromagnetic Hartree-Fock band structure (Ref. 33) these authors added a self-energy constructed within the local approximation to three-body scattering theory. The obtained band structures show the same “large scale features” as the one obtained here, but there are also significant differences, particularly so near the top of the valence band. More detailed comparison with experiment seems necessary to discuss the merits of the various theories.

Next, there is a clear analogy between the present theory and the cluster method of Fujimori and Minami¹¹ and *va Elp et al.*¹² With the exception of $d^9 \underline{L}^2$ states in the photoemissions spectrum the present theory employs the same type of basis states as the cluster calculations. The only difference is that we designate one of the degenerate ground states of d^n as a “vacuum state” and interpret the other states as “deviations” from this vacuum state. Those deviations which carry the quantum number of an electron then are considered as effective free Fermions. As discussed above, the low density of these effective Fermions probably make this a very good approximation.

There is also an obvious relationship between the present theory and the work of Unger and Fulde.³⁴ Using the projection technique developed by Becker and Fulde³⁵ these authors constructed an equation of motion for single-particle spectral functions of the CuO_2 plane, which is very similar to the ones which would be obtained from our effective Hamiltonians. Finally we address the work of Bala *et al.*,²¹ which is very similar in spirit to the present theory. These authors derived a “Kondo-Heisenberg”-like model operating in the subspace of $d^8 \underline{L}$ type states by eliminating, via canonical transformation, the charge fluctuations between states of the type (${}^3A_{2g} d^8$) \underline{L} and states of the type d^7 (their theory was concerned with the motion of a single hole in an $\text{O}2p$ orbital). Accordingly, their theory produced (in addition to the free-electron-like $\text{O}2p$ bands) two weakly dispersive bands, one for each of the “flavors” e_g and t_{2g} whereby the flavor stands for the symmetry of the linear combination of $\text{O}2p$ orbitals around a given Ni site. Thereby Bala *et al.* actually went one step beyond the present theory by taking into account the coupling of $\text{O}2p$ -like holes to the antiferromagnetic magnons, which is omitted in the present theory. In the present theory, no canonical transformation is performed, so that also the high energy features (satellite and upper Hubbard band) are reproduced. Moreover, we also take the excited multiplets of d^8 and their covalent mixing with the d^7 multiplets into account, whence we obtain a larger number of ZRS-like bands, consistent with experiment. Experimentally the impact of the coupling to magnons which is ignored in the present theory but treated accurately in the work of Bala *et al.* could be studied only by considering the “fine structure” of the broad peak at the valence band top. These states seem to have an appreciable dispersion which might or might not be influenced by the coupling to magnons.

- ¹W. Kohn and L. J. Sham, Phys. Rev. **140**, A1133 (1965).
- ²K. Terakura, T. Oguchi, A. R. Williams, and J. Kubler, Phys. Rev. B **30**, 4734 (1984).
- ³G. A. Sawatzky and J. W. Allen, Phys. Rev. Lett. **53**, 2339 (1984).
- ⁴M. R. Norman and A. J. Freeman, Phys. Rev. B **33**, 8896 (1986).
- ⁵A. Svane and O. Gunnarsson, Phys. Rev. Lett. **65**, 1148 (1990).
- ⁶Z. Szotek, W. M. Temmerman, and H. Winter, Phys. Rev. B **47**, 4029 (1993).
- ⁷V. I. Anisimov, J. Zaanen, and O. K. Andersen, Phys. Rev. B **44**, 943 (1991).
- ⁸V. I. Anisimov, I. V. Solovyev, M. A. Korotin, M. T. Czyzyk, and G. A. Sawatzky, Phys. Rev. B **48**, 16 929 (1993).
- ⁹F. Aryasetiawan and O. Gunnarsson, Phys. Rev. Lett. **74**, 3221 (1995).
- ¹⁰S. Massidda, A. Continenza, M. Posternak, and A. Baldereschi, Phys. Rev. B **55**, 13 494 (1997).
- ¹¹A. Fujimori and F. Minami, Phys. Rev. B **30**, 957 (1984).
- ¹²J. van Elp, H. Eskes, P. Kuiper, and G. A. Sawatzky, Phys. Rev. B **45**, 1612 (1992).
- ¹³J. Hubbard, Proc. R. Soc. London, Ser. A **237**, 277 (1964); **281**, 401 (1964).
- ¹⁴D. Senechal, D. Perez, and M. Pioro-Ladriere, Phys. Rev. Lett. **84**, 522 (2000).
- ¹⁵D. Senechal, D. Perez, and D. Plouffe, Phys. Rev. B **66**, 075129 (2002).
- ¹⁶F. C. Zhang and T. M. Rice, Phys. Rev. B **37**, 3759 (1988).
- ¹⁷J. Zaanen, G. A. Sawatzky, and J. W. Allen, Phys. Rev. Lett. **55**, 418 (1985).
- ¹⁸S.-J. Oh, J. W. Allen, I. Lindau, and J. C. Mikkelsen, Jr., Phys. Rev. B **26**, 4845 (1982).
- ¹⁹O. Tjernberg, S. Söderholm, U. O. Karlsson, G. Chiaia, M. Qvarford, H. Nylén, and I. Lindau, Phys. Rev. B **53**, 10 372 (1996).
- ²⁰L. H. Tjeng, C. T. Chen, J. Ghijsen, P. Rudolf, and F. Sette, Phys. Rev. Lett. **67**, 501 (1991).
- ²¹J. Bala, A. M. Oles, and J. Zaanen, Phys. Rev. Lett. **72**, 2600 (1994); J. Bala, A. M. Oles, and J. Zaanen, Phys. Rev. B **61**, 13 573 (2000).
- ²²H. Kuhlenbeck, G. Odörfer, R. Jaeger, G. Illing, M. Menges, Th. Mull, H.-J. Freund, M. Pöhlichen, V. Staemmler, S. Witzel, C. Scharfschwerdt, K. Wennemann, T. Liedtke, and M. Neumann, Phys. Rev. B **43**, 1969 (1991).
- ²³Z. X. Shen, R. S. List, D. S. Dessau, B. O. Wells, O. Jepsen, A. J. Arko, R. Bartlett, C. K. Shih, F. Parmigiani, J. C. Huang, and P. A. P. Lindberg, Phys. Rev. B **44**, 3604 (1991).
- ²⁴R. Eder, O. Rokojanu, and G. A. Sawatzky, Phys. Rev. B **58**, 7599 (1998).
- ²⁵A. Dorneich, M. G. Zacher, C. Gröber, and R. Eder, Phys. Rev. B **61**, 12 816 (2000).
- ²⁶M. G. Zacher, R. Eder, E. Arrigoni, and W. Hanke, Phys. Rev. B **65**, 045109 (2002).
- ²⁷O. K. Andersen, Phys. Rev. B **12**, 3060 (1975).
- ²⁸R. G. Shulman and S. Sugano, Phys. Rev. **130**, 506 (1963).
- ²⁹V. N. Kotov, O. Sushkov, Z. Weihong, and J. Oitmaa, Phys. Rev. Lett. **80**, 5790 (1998).
- ³⁰J. B. Goodenough, Phys. Rev. **100**, 564 (1955); J. Phys. Chem. Solids **6**, 287 (1958); J. Kanamori, *ibid.* **10**, 87 (1959).
- ³¹M. Potthoff, M. Aichhorn, and C. Dahnken, Phys. Rev. Lett. **91**, 206402 (2003).
- ³²F. Manghi, C. Calandra, and S. Ossicini, Phys. Rev. Lett. **73**, 3129 (1994).
- ³³M. Takahashi and J. I. Igarashi, Phys. Rev. B **54**, 13 566 (1996); Ann Phys. **5**, 247 (1996).
- ³⁴P. Unger and P. Fulde Phys. Rev. B **47**, 8947 (1993); **48**, 16 607 (1993); **51**, 9245 (1995).
- ³⁵K. W. Becker and P. Fulde, Z. Phys. B: Condens. Matter **72**, 423 (1988); K. W. Becker and W. Brening, *ibid.* **79**, 195 (1990).